Published in final edited form as:

J Am Soc Mass Spectrom. 2017 September ; 28(9): 1805–1814. doi:10.1007/s13361-017-1710-3.

The Impact of Phosphorylation on Electron Capture Dissociation of Proteins: A Top-down Perspective

Bifan Chen[a], **Xiao Guo**[a], **Trisha Tucholski**[a], **Ziqing Lin**[b], **Sean McIlwain**[c,d], and **Ying Ge**[a,b,e,*]

[a]Department of Chemistry, University of Wisconsin-Madison, Madison, WI, USA

[b]Department of Cell and Regenerative Biology, School of Medicine and Public Health, University of Wisconsin-Madison, Madison, WI, USA

[c]Department of Biostatistics and Medical Informatics, University of Wisconsin-Madison, Madison, WI, USA

[d]UW Carbone Cancer Center, School of Medicine and Public Health, University of Wisconsin-Madison, Madison, WI, USA

[e]Human Proteomics Program, School of Medicine and Public Health, University of Wisconsin-Madison, Madison, WI, USA

Abstract

Electron capture dissociation (ECD) is well suited for the characterization of phosphoproteins, with which labile phosphate groups are generally preserved during the fragmentation process. However, the impact of phosphorylation on ECD fragmentation of intact proteins remains unclear. Here, we have performed a systematic investigation of the phosphorylation effect on ECD of intact proteins by comparing the ECD cleavages of mono-phosphorylated α-casein, multi-phosphorylated β-casein, and immunoaffinity-purified phosphorylated cardiac troponin I with those of their unphosphorylated counterparts, respectively. In contrast to phosphopeptides, phosphorylation has significantly reduced deleterious effects on the fragmentation of intact proteins during ECD. On a global scale, the fragmentation patterns are highly comparable between unphosphorylated and phosphorylated precursors under the same ECD conditions, despite a slight decrease in the number of fragment ions observed for the phosphorylated forms. On a local scale, single phosphorylation of intact proteins imposes minimal effects on fragmentation near the phosphorylation sites, but multiple phosphorylations in close proximity result in a significant reduction of ECD bond cleavages.

Graphical abstract

Address reprint requests to: Dr. Ying Ge, 1300 University Ave., SMI 130, Madison, Wisconsin, USA. Tel: 608-263-9212, Fax: 608-265-5512, ge2@wisc.edu.

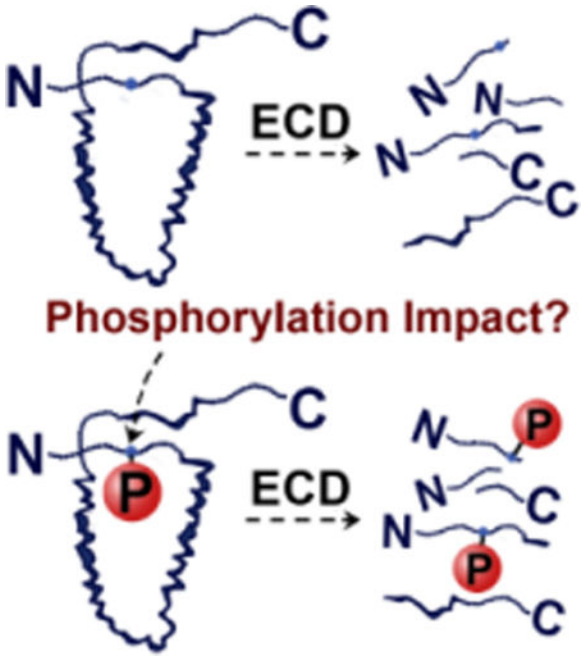

Keywords

Phosphorylation; Mass Spectrometry; Electron Capture Dissociation; Top-down MS

Introduction

Since the introduction of electron capture dissociation (ECD) in 1998 [1], this powerful tandem mass spectrometry (MS/MS) technique has been widely used to elucidate amino acid sequences, structures, and, particularly, to localize post-translational modifications (PTMs) of proteins [2–6]. During ECD, ion analytes (proteins or peptides) are irradiated by low-energy electrons, cleaving N-C_α bonds and producing ***c***-type and ***z***-type ions [1, 2, 7, 8]. Compared to traditional “slow heating” MS/MS methods such as collisionally activated dissociation (CAD) [9, 10] and infrared multi-photon dissociation (IRMPD) [11], which usually cleave the weakest bonds in a given protein/peptide ion and lead to the preferred loss of labile PTMs, ECD causes fast fragmentation prior to energy randomization over the whole protein or peptide [1, 12–14]. This characteristic of ECD generally results in preservation of labile PTMs [2, 15], such as phosphorylation [16] and OGlcNAc [17].

Phosphorylation, a highly prevalent PTM, plays a critical role in regulating various complex cellular processes, and altered phosphorylation is implicated in many diseases [5, 6, 18]. During CAD, the phosphorylated ions often experience 98 and 80 Da neutral losses, hindering the interrogation of phosphorylation sites [19]. In contrast, ECD preserves phosphorylation while providing rich fragmentation patterns, presenting a valuable option to characterize both phosphopeptides and phosphoproteins [16]. For phosphopeptides, it has been demonstrated that ECD can be applied in data dependent online LC-MS/MS experiments for large scale identification and localization of phosphorylation sites [20].

However, because of the elongated ion accumulation time, utilization of ECD in online LC-MS/MS is not widely utilized [21]. On the other hand, ECD is particularly powerful in characterizing phosphoproteins in an offline mode. Over the past years, our group has successfully applied Fourier transform ion cyclotron resonance mass spectrometry (FT-ICR MS) equipped with ECD to comprehensively characterize biologically important phosphoproteins in the heart such as myosin binding protein C [22], cardiac troponin I [23–25], tropomyosin [26, 27], and AMPactivated protein kinase catalytic domain [28]. Furthermore, we were able to discover reduced phosphorylation of a previously unknown phosphoprotein, enigma homolog isoform 2, from swine heart tissue after acute myocardial infarction and localize the phosphorylation site with ECD [29], which demonstrated the power of ECD for characterizing phosphoproteins.

In addition to localizing phosphorylation sites, ECD has also proven feasibility for quantitative analysis. The Kelleher group has pioneered and demonstrated the use of ECD spectra to quantify isomeric methylated and acetylated proteoforms from histone H4 [30]. Our group has also developed a novel strategy to quantify isomeric phosphorylated proteins that utilized only the abundance of unphosphorylated fragment ions with intraspectrum normalization, which avoids confronting potential influence from the phosphate groups on the ECD [31]. However, the influence of phosphorylation on intact protein ECD fragmentation is still largely unknown. Although Creese and Cooper showed that the addition of phosphorylation has deleterious effect on ECD sequence coverage for doubly charged peptides [32], and later demonstrated that the structure rather than the sequence of phosphopeptides influences ECD efficiency [33], these results could not be generalized to proteins. Compared with peptides, the physiochemical properties for larger intact proteins tend to be much less affected by the addition of phosphorylation, thus prompting further investigation.

Here, we have systematically investigated the potential effect of phosphorylation of intact proteins on ECD behavior using mono-phosphorylated α-casein, multi-phosphorylated β-casein, and immunoaffinity-purified cardiac troponin I from swine and rhesus monkey tissues. We have localized the phosphorylation sites and statistically compared the ECD fragments of the unphosphorylated and the phosphorylated forms of these proteins. The results collectively show that the phosphorylation has considerably less deleterious influence on ECD fragmentation of intact protein compared to peptides. Globally, the total number of fragment ions produced by ECD was slightly decreased for the phosphorylated precursor ions, but the fragmentation pattern remained highly comparable between the unphosphorylated and the phosphorylated proteins. Locally, near the amino acid residues adjacent to the single phosphorylation site, fragmentation patterns remained largely unchanged; however, multiple phosphorylations in close proximity led to a decrease in protein backbone cleavages. These findings provide a contemporary top-down perspective on ECD fragmentation of phosphoproteins.

Experimental

Chemicals and reagents

Dephosphorylated α-casein (bovine milk) was purchased from Sigma-Aldrich (St. Louis, MO, USA). β-Casein (bovine pancreas) standard was purchased from Protea Biosciences (Morgantown, WV, USA). Lambda protein phosphatase (λPP) was purchased from New England Biolabs (Ipswich, MA, USA). Pierce Protein Concentrator PES, 10K MWCO, high-performance liquid chromatography (HPLC)-grade water (H2O), and acetonitrile (ACN) were purchased from Fisher Scientific (Waltham, MA, USA). All other reagents were purchased from Sigma-Aldrich unless otherwise specified.

In vitro dephosphorylation of β-casein

For every 20 μL of dephosphorylation reaction, 10 μg of β-casein was incubated with 100 units of lambda protein phosphatase (λPP) with the supplement of 1 mM $MnCl_2$ in 1× protein metallophosphatase buffer. The mixture was incubated at 30 °C for 0.5 h. Subsequently, dephosphorylated β-casein was desalted using 0.1% formic acid in H2O wash through 10 K MWCO protein concentrators prior to top-down MS analysis. The final concentrations of the phosphorylated and the unphosphorylated β-casein were about 0.25 μg/μL in ACN: H2O (50:50) and 0.1% formic acid.

Immunoaffinity purification of swine and rhesus monkey cTnI

Heart tissue was obtained from juvenile Yorkshire domestic pig and rhesus monkey hearts as approved by the University of Wisconsin Animal Care and Use Committee. The excised heart tissue was immediately frozen in liquid nitrogen and stored in a – 80 °C freezer. The whole cardiac troponin complex was purified by the immunoaffinity purification method as previously described [34, 35]. Briefly, 1.5 g of heart tissue was homogenized in tissue wash buffer (NaH_2PO_4 500 mM, Na_2HPO_4 100 mM, $MgCl_2$ 100 mM, EGTA 100 mM, NaCl 0.1 M, Triton X-100 1%, DTT 5 mM, protease and phosphatase inhibitor cocktail tablet, PMSF 1 mM, leupeptin 2 μg/mL, pH 7.4) using a Polytron electric homogenizer (Model PRO200, PRO Scientific Inc., Oxford, CT, USA) for 30 s on ice. The homogenate was centrifuged at 8000 rpm at 4 °C for 10 min; the pellet was collected and resuspended in 6 mL protein extraction buffer (0.7 M LiCl, 25 mM Tris, 5 mM EGTA, 0.1 mM $CaCl_2$, 5 mM DTT, 1 mM PMSF, 2 μg/mL leupeptin, and 0.75 mg/mL protease and phosphatase inhibitor cocktail, pH 8.0) and protein extraction was performed with agitation on a nutating mixer (Fisher Scientific Inc., Pittsburgh, PA, USA) at 4 °C for 45 min. The sample was then centrifuged at 16,000 rpm (Centrifuge 5415R; Eppendorf, Hamburg, Germany) for 5 min. The supernatant was further centrifuged at 55,000 rpm (Beckman L-55 ultracentrifuge; Beckman Coulter, Fullerton, CA, USA) for 45 min to completely remove any particulate. The supernatant was incubated with 0.25 mL of CNBr-activated Sepharose CL-4B conjugated with 1.25 mg monoclonal cTnI antibody (anti-troponin I monoclonal antibody MF4 and 14G5; HyTest Ltd., Turku, Finland) for 35 min at 4 °C to ensure complete binding of troponin complex to the antibody. After washing the column with 2 mL of extraction buffer, the bound troponin complex was eluted with 100 mM glycine at pH 2 into four 0.4 mL fractions and neutralized immediately with 40 μL of 1M MOPS (pH 9). Fractions were further separated and desalted

using an offline reverse phase protein microtrap (Michrom Bioresources Inc., Auburn, CA, USA) to obtain purified cTnI.

Top-down MS analysis

A 7T linear ion trap/Fourier transform ion cyclotron resonance (FT-ICR) mass spectrometer (MS) (LTQ/FT Ultra, Thermo Scientific, Bremen, Germany) and a 12T SolariX FTICR-MS (Bruker, Bremen, Germany) equipped with ECD were used for the investigation. Triversa NanoMate (Advion, Ithaca, NY, USA), a chip-based nano-electrospray ionization (nanoESI) system delivered all samples into the mass spectrometers. For the LTQ/FT Ultra, the resolving power was set to 200,000 at 400 m/z. During ECD, individual precursor ions with the same charge state of the unphosphorylated and the phosphorylated proteins were isolated and fragmented using 2.2%–3.3% electron energy with a 50 ms duration and no delay; 1000 to 9000 transients were averaged to ensure high quality of ECD spectra. For the SolariX FTICR-MS, the mass spectra were collected over a 202.76 to 3000 m/z range with 2 mega-words (resolution 270,000 at 400 m/z) transient length (1.1534 s) and a pulse at 20% excitation power. All MS/MS spectra were accumulated for 1000 scans unless specified otherwise. For the “standard” parameters, ECD pulse length was set to 0.05 s; ECD bias was set to 0.8 V (0.8 eV); and ECD lens was 10 V for ECD fragmentation.

Data Analysis

MASH Suite [36] and MASH Suite Pro [37] were used to analyze MS/MS data generated from 7T LTQ/FT Ultra and 12 T SolariX FT-ICR, respectively. All peaks were extracted with a signal-to-noise ratio set to 3 and a minimum fit of 60%, followed by manual validation. Fragment ions were assigned by matching the experimental fragment ions to the calculated ones from theoretical amino acid sequence with a 10 ppm mass tolerance. The abundance of each ion is the sum of the intensities from the top five most abundant isotopomers. Subsequently, the quantitation value was normalized to the charge of the ion. The normalized values from the same ions with different charge states were then summed. The relative abundance of each fragment ion was calculated by normalizing to the most abundant fragment ion within the same spectrum.

Results and Discussion

To evaluate the phosphorylation effect on ECD fragmentation of intact protein, it is critical to maintain phosphorylation as the only changing factor and minimize other variations arising from instrument parameters and sample introduction. ECD parameters were kept constant between ECD of unphosphorylated and phosphorylated counterparts of the same protein. Because the precursor ion signal in the FTMS instrument may introduce biased fragment ion intensity, the ion accumulation was adjusted between the isolated unphosphorylated and phosphorylated precursor so that their intensities are comparable in a single scan. Furthermore, fragment ion intensity was normalized to the most abundant fragment ion in each spectrum to minimize the variation caused by the difference in precursor ion intensity. Here, three different protein species, including single and multiple phosphorylation sites with multiple replicates, were used to investigate the influence of phosphorylation on ECD of intact protein.

ECD of mono-phosphorylated vs. unphosphorylated α-casein

We first acquired MS spectra on the LTQ/FT of the commercially available "dephosphorylated" α-casein (M_r 22960.48 Da) after desalting by offline reverse-phase chromatography. The MS spectrum reveals the detection of unphosphorylated α- casein with the presence of mono-phosphorylated (major) and the bis-phosphorylated (minor) forms (Figure 1a). The monophosphorylated precursor was subsequently isolated for ECD to localize the phosphorylation site. After validation of all fragment ions, a match to the theoretical α-casein sequence (UniProtKB-P02662) provides two possible phosphorylation sites, Ser88 and Ser115 (Figure 1b). One hundred and 108 out of 198 backbone bonds were cleaved when the phosphorylation was assigned to Ser88 and Ser115, respectively. Careful manual validation of fragment ions resulting from ECD (Figure 1c and Supplementary Figure S1) further confirmed the heterogeneity of the mono-phosphorylated α-casein. Specifically, representative ions $\boldsymbol{c}_{88}$, $\boldsymbol{c}_{92}$, $\boldsymbol{c}_{93}$, and $\boldsymbol{c}_{105}$ all coexisted with the monophosphorylated counter parts (Figure 1c). Prior to residue Asp85, no phosphorylated ions were observed as demonstrated by $\boldsymbol{c}_{54}$, $\boldsymbol{c}_{74}$, $\boldsymbol{c}_{83}$, and $\boldsymbol{c}_{85}$ (Supplementary Figure S1). Furthermore, the presence of only the mono-phosphorylated forms of $\boldsymbol{c}_{118}$, $\boldsymbol{c}_{132}$, and $\boldsymbol{c}_{144}$ ions without the detection of the unphosphorylated counterparts proved the absence of phosphorylation sites after Glu118. Therefore, with only two possible serine residues from Asp85 to Glu118, we confidently assigned the mono-phosphorylation site to Ser88 and Ser115, with the latter being the predominant form.

The unphosphorylated and the mono-phosphorylated α- casein from the same charge state were then isolated and subjected to ECD. Because ECD of precursor ions with higher charge states provide more extensive fragmentation [38], charge state 23^+ was selected for the study. Nine different spectra of unphosphorylated and monophosphorylated α-casein with transients up to 9000 were used to ensure data quality and maximum sequence coverage. The number of observed ions increases as the number of transients accumulated increases (Supplementary Figure S2), because averaging more data points resolves low abundance ions. Therefore, we analyzed spectra collected at the plateau area, where more transients do not provide as many additional observed ions. Consequently, the potential variation introduced by differences in data accumulation time and noise was minimized. Relative abundance of the $\boldsymbol{c}$ and $\boldsymbol{z}^{\bullet}$ fragment ions from the unphosphorylated (top) and monophosphorylated (bottom) precursors (23^+) normalized to the most abundant product ion were plotted against their corresponding cleavage sites (Figure 2). Globally, for the $\boldsymbol{c}$ ions, the cleavage patterns of the unphosphorylated and the monophosphorylated were similar, indicating a negligible effect of the single phosphorylation on ECD fragmentation efficiency of α-casein (Figure 2a). However, the total number of the $\boldsymbol{z}^{\bullet}$ ions was smaller compared with the c ions for both the unphosphorylated and phosphorylated forms. Furthermore, ECD of the unphosphorylated form provided more $\boldsymbol{z}^{\bullet}$ ions (77 $\boldsymbol{z}^{\bullet}$ ions) than that of the mono-phosphorylated form (61 $\boldsymbol{z}^{\bullet}$ ions), resulting in more cleavages (Figure 2b). A closer examination of cleavage sites adjacent to the phosphorylation site at Ser115 revealed similar fragmentation patterns for the unphosphorylated and the mono-phosphorylated α-casein. While the cleavage patterns remained mostly identical around the phosphorylation site Ser115, the N–C_α bond (at Leu120) that produces fragments $\boldsymbol{c}_{120}$ and $\boldsymbol{z}^{\bullet}_{89}$ was not cleaved in the unphosphorylated form (Figure 2a and b insert). However, the interpretation of these

results was complicated by positional isomers. Additionally, the number and position of phosphorylation sites on an intact protein also potentially influence ECD fragmentation. Therefore, further investigation was conducted using β-casein.

ECD of multi-phosphorylated vs. unphosphorylated β-casein

β-Casein (M_r 23568.32 Da) from bovine pancreas has five phosphorylation sites, with four (Ser15, Ser17, Ser18, and Ser19) clustered together and one (Ser35) further away from the N-terminal, making it a well-suited model for probing the potential influence of both the number and the location of the phosphorylation. We first assessed the reproducibility of the ECD fragmentation using identical ECD parameters (a "standard" setting: 0.8 eV for electron energy and 50 ms for electron irradiation time) on 10 replicates of the fully phosphorylated β-casein. As shown in Figure 3a, the ECD spectra from all three replicates demonstrate nearly identical reduced precursor ion and product ion patterns. The relative abundances of representative fragment ions from all 10 replicates were plotted and grouped into unphosphorylated ***c*** ions (Figure 3b), phosphorylated ***c*** ions (Figure 3c), and unphosphorylated $\boldsymbol{z}^{\bullet}$ ions (Figure 3d). Regardless of the addition of phosphorylations, the relative abundance of these ***c*** and $\boldsymbol{z}^{\bullet}$ ions are highly consistent with a small standard error of the mean (SEM) within 4%. In general, smaller ions have relatively smaller SEM compared with larger ions since ions with higher molecular weight tend to exhibit lower signal-to-noise ratios and may undergo secondary fragmentations. The SEM of the larger ions can be minimized by accumulating more scans (data not shown). The highly reproducible ECD fragment patterns among multiple replicates allow us to confidently utilize one ECD experiment for each set of parameters to further evaluate its performance on phosphorylated β-casein compared with the unphosphorylated form.

Using the standard parameters, the 23^+ charge state ions of the unphosphorylated and the phosphorylated β-casein were isolated individually for ECD on two different FTMS instruments, Thermo 7T LTQ/FT and Bruker 12T solariX FT-ICR MS (Figure 4 and Supplementary Figure S3). The MS isolation of charge state 23^+ of the unphosphorylated and the phosphorylated β-casein demonstrated the existence of five phosphorylations (Δ = 399.79 Da) for the phosphorylated form and confirmed the completeness of the dephosphorylation assay (Figure 4a). Figure 4b and c depict the resulting fragmentation maps of the unphosphorylated and the phosphorylated β-casein after matching to the theoretical sequence of β-casein (UniProtKB-P02666). Overall, 144 and 138 of the 208 backbone bonds were cleaved from the unphosphorylated and the phosphorylated β-casein respectively; 92 ***c*** ions and 109 $\boldsymbol{z}^{\bullet}$ ions from the unphosphorylated β-casein, and 88 ***c*** ions and 106 $\boldsymbol{z}^{\bullet}$ ions from the phosphorylated β-casein, were observed. Although ECD of the phosphorylated form exhibited slightly fewer ions, the cleavages were highly comparable between the phosphorylated and the unphosphorylated β-casein. Comparison of the relative abundance of ***c*** ions and $\boldsymbol{z}^{\bullet}$ ions (Figure 4 d and e) further affirms the highly similar cleavage patterns, with only a few unmatched ions between the unphosphorylated (top) and phosphorylated counterparts (bottom). Most of the unmatched ions that were found in the unphosphorylated but not the phosphorylated β-casein were located near the highly phosphorylated area of the sequence surrounding phosphorylation sites at Ser15, Ser17, Ser18, and Ser19 (Figure 4d). This discrepancy could suggest that multiple phosphorylations

existing in close proximity hinder ECD fragmentation. However, it is more likely that the introduction of negative charges from the multiple phosphorylated residues alters the overall positive charge of the product ions, as an extra positive charge from the basic residue Arg25 seems to alleviate this problem and resulted in the cleavage of the next ***c*** ion, $\boldsymbol{c}_{25}$. On the other hand, cleavages around the phosphorylated Ser35 were not compromised, with every N–Cα bond within nine residues before and after Ser35 cleaved ($\boldsymbol{c}_{25}$ to $\boldsymbol{c}_{45}$), suggesting that a single phosphorylation results in minimal influence on ECD fragmentation of the intact protein.

ECD of mono-phosphorylated vs. unphosphorylated cardiac troponin I from swine and rhesus monkey

Cardiac troponin I (cTnI) was immunoaffinity-purified from swine (M_r 23919.72 Da) and rhesus monkey (M_r 23849.79 Da) tissue lysate followed by offline reverse phase desalting as described previously [25, 34]. Similarly, we compared the relative abundance of fragment ions produced by ECD of the unphosphorylated (top) and phosphorylated (bottom) forms of endogenous cardiac troponin I from swine (phosphorylation site at Ser22), and from rhesus monkey (phosphorylation site at Ser23) (Figure 5a, b). Globally, 106 out of 209 backbone bonds were cleaved in the unphosphorylated swine cTnI, and 100 were cleaved from the mono-phosphorylated form. The total number of ***c*** ions and $\boldsymbol{z}^{\bullet}$ ions from the unphosphorylated compared with the mono-phosphorylated swine cTnI was 47 to 46 and 62 to 54, respectively. Near the phosphorylation site (Ser22), the number of ***c*** ions between $\boldsymbol{c}_{18}$ to $\boldsymbol{c}_{28}$ from the unphosphorylated compared with the mono-phosphorylated swine cTnI was 10 to 10 (Supplementary Table S1). Similar findings were observed in the comparison of unphosphorylated and mono-phosphorylated cTnI from rhesus (Figure 5b), as the number of c ions between $\boldsymbol{c}_{18}$ to $\boldsymbol{c}_{28}$ from the unphosphorylated compared with the mono-phosphorylated rhesus monkey cTnI was also 10 to 10 near the phosphorylation site (Ser23). These results reiterate that although the overall number of total fragments is slightly decreased, a single phosphorylation event has a minimal influence on ECD fragmentation efficiency near the phosphorylation site of an intact protein.

The effect of phosphorylation on ECD of protein vs. peptide ions

Compared with peptides, intact proteins are much larger in size and, therefore, the addition of one or more phosphorylations is less likely to perturb the overall ion behavior during ECD. We demonstrated that, locally, adjacent to the phosphorylation site, ECD cleavages remain similar between mono-phosphorylated and unphosphorylated proteoforms. However, due to the introduction of a negatively charged moiety (deprotonated phosphate group), phosphorylated protein ions still experience different fragmentation than unphosphorylated counterparts even with selection of the same charge state for fragmentation. This becomes more apparent when multiple phosphorylations are present in close proximity on a protein. For the case of the multiply phosphorylated versus unphosphorylated β-casein, ECD fragmentation was greatly reduced at the region surrounding the multiple phosphorylation sites. In a previous study, Creese and Cooper investigated the ECD efficiency on phosphopeptides using a peptide from β- casein (Phe33 to Lys48; phosphorylated Ser35) [32]. They found that the phosphorylated peptide did not fragment as well as the unphosphorylated counterpart, and postulated that the phosphorylation alters peptide folding

through the formation of salt-bridges between the glutamine and the glutamic acid residues. Using a very high electron energy, they were able to cleave 13 out of the 15 N–C_α bonds on the phosphopeptide. In our case, ECD cleaved all of the previously mentioned 15 N-C_α bonds around Ser35 (Figure 4b) of the phosphorylated β- casein with low electron energy. Nevertheless, in contrast to peptide ions, protein ions carry significantly more charges in denatured conditions, which not only disturbs electrostatic interaction (salt bridges) [39, 40], but also increases ECD reaction cross-section [15], resulting in minor differences in the overall ECD cleavages between the phosphorylated and the unphosphorylated species without the requirement of additional electron energy as for phosphopeptides [32]. Our data also suggests that globally, ECD of the phosphorylated form generally produces slightly fewer fragment ions; however, it is drastically less affected by phosphorylation compared with the marked effects observed for phosphopeptides.

Conclusion

In this study, we systematically investigated the influence of phosphorylation on ECD fragmentation of intact proteins, including mono-phosphorylated α-casein, multiply phosphorylated β-casein, and immunoaffinity-purified cardiac troponin I from swine and rhesus monkey, by analyzing the relative ion abundance from the unphosphorylated and the phosphorylated forms under the same ECD conditions. The results suggest that compared with phosphopeptides, phosphorylation has little deleterious effect on ECD fragmentation of intact proteins. Globally, phosphorylation on intact proteins slightly decreases the total number of fragment ions, but the pattern of fragmentation remains highly similar. Locally, phosphorylation on intact proteins tends not to significantly affect the fragmentation and cleavages of the amino acid residues adjacent to the phosphorylation sites; however, when multiple phosphorylations are present in close proximity, cleavages near the phosphorylation sites decrease.

Supplementary Material

Refer to Web version on PubMed Central for supplementary material.

Acknowledgments

This work is dedicated to Professor Kristina Håkansson, the recipient of the 2016 Biemann Medal of the ASMS, for her outstanding achievement in the field of mass spectrometry related to electron-based activation methods. The authors thank Fangmin Xu, Han Zhang, and Huseyin Guner on the initial studies on the LTQ/FT. They thank Jeremy Wolff from Bruker for technical assistance on the Solarix FTMS. They also thank Dr. Barbara Lewis and Zachery Gregorich for critical reading of the manuscript. Financial support was kindly provided by NIH R01HL109810 and HL096971 (to Y.G.) and GM117058 (to Song Jin and Y.G.). They also acknowledge NIH high-end instrument grant S10OD018475 (to Y.G.). T.T. acknowledges support of the NIH Chemical Biology Interface Training grant NIH T32GM008505.

Abbreviations

PTMs	post-translational modifications
ESI	electrospray ionization
FT-ICR	Fourier transform ion cyclotron resonance

MS	mass spectrometry
CAD	collisionally activated dissociation
IRMPD	Infrared multi-photon dissociation
ECD	electron capture dissociation
MS/MS	tandem mass spectrometry
O-GlcNAc	O-Linked β-N-acetylglucosamine
cTnI	Cardiac troponin I

References

1. Zubarev RA, Kelleher NL, McLafferty FW. Electron capture dissociation of multiply charged protein cations. A nonergodic process. J Am Chem Soc. 1998; 120:3265–3266.
2. Cooper HJ, Hakansson K, Marshall AG. The role of electron capture dissociation in biomolecular analysis. Mass Spectrom Rev. 2005; 24:201–222. [PubMed: 15389856]
3. Zhang H, Ge Y. Comprehensive analysis of protein modifications by top-down mass spectrometry. Circ-Cardiovasc Genet. 2011; 4:711–720. [PubMed: 22187450]
4. Schennach M, Breuker K. Probing Protein Structure and Folding in the Gas Phase by Electron Capture Dissociation. J Am Soc Mass Spectrom. 2015; 26:1059–1067. [PubMed: 25868904]
5. Gregorich ZR, Ge Y. Top-down proteomics in health and disease: challenges and opportunities. Proteomics. 2014; 14:1195–1210. [PubMed: 24723472]
6. Cai WX, Tucholski TM, Gregorich ZR, Ge Y. Top-down proteomics: technology advancements and applications to heart diseases. Expert Rev Proteomics. 2016; 13:717–730. [PubMed: 27448560]
7. Zubarev RA, Kruger NA, Fridriksson EK, Lewis MA, Horn DM, Carpenter BK, McLafferty FW. Electron capture dissociation of gaseous multiply-charged proteins is favored at disulfide bonds and other sites of high hydrogen atom affinity. J Am Chem Soc. 1999; 121:2857–2862.
8. Zhurov KO, Fornelli L, Wodrich MD, Laskay UA, Tsybin YO. Principles of electron capture and transfer dissociation mass spectrometry applied to peptide and protein structure analysis. Chem Soc Rev. 2013; 42:5014–5030. [PubMed: 23450212]
9. Williams ER, Furlong JJ, McLafferty FW. Efficiency of collisionally-activated dissociation and 193-nm photodissociation of peptide ions in fourier transform mass spectrometry. J Am Soc Mass Spectrom. 1990; 1:288–294. [PubMed: 24248821]
10. Senko MW, Speir JP, Mclafferty FW. Collisional activation of large multiply-charged ions using fourier-transform mass-spectrometry. Anal Chem. 1994; 66:2801–2808. [PubMed: 7978294]
11. Little DP, Paul Speir J, Senko MW, O'Connor PB. Infrared multiphoton dissociation of large multiply charged ions for biomolecule sequencing. Anal Chem. 1994; 66:2809–2815. [PubMed: 7526742]
12. Breuker K, Oh HB, Lin C, Carpenter BK, McLafferty FW. Nonergodic and conformational control of the electron capture dissociation of protein cations. Proc Natl Acad Sci U S A. 2004; 101:14011–14016. [PubMed: 15381764]
13. McLafferty FW, Horn DM, Breuker K, Ge Y, Lewis MA, Cerda B, Zubarev RA, Carpenter BK. Electron capture dissociation of gaseous multiply charged ions by Fourier-transform ion cyclotron resonance. J Am Soc Mass Spectrom. 2001; 12:245–249. [PubMed: 11281599]
14. Zubarev RA. Reactions of polypeptide ions with electrons in the gas phase. Mass Spectrom Rev. 2003; 22:57–77. [PubMed: 12768604]
15. Zubarev RA, Horn DM, Fridriksson EK, Kelleher NL, Kruger NA, Lewis MA, Carpenter BK, McLafferty FW. Electron capture dissociation for structural characterization of multiply charged protein cations. Anal Chem. 2000; 72:563–573. [PubMed: 10695143]

16. Shi SDH, Hemling ME, Carr SA, Horn DM, Lindh I, McLafferty FW. Phosphopeptide/phosphoprotein mapping by electron capture dissociation mass spectrometry. Anal Chem. 2001; 73:19–22. [PubMed: 11195502]
17. Mirgorodskaya E, Roepstorff P, Zubarev RA. Localization of O-glycosylation sites in peptides by electron capture dissociation in a Fourier transform mass spectrometer. Anal Chem. 1999; 71:4431–4436. [PubMed: 10546526]
18. Mann M, Ong SE, Gronborg M, Steen H, Jensen ON, Pandey A. Analysis of protein phosphorylation using mass spectrometry: deciphering the phosphoproteome. Trends Biotechnol. 2002; 20:261–268. [PubMed: 12007495]
19. Steen H, Jebanathirajah JA, Rush J, Morrice N, Kirschner MW. Phosphorylation analysis by mass spectrometry: myths, facts, and the consequences for qualitative and quantitative measurements. Mol Cell Proteomics. 2006; 5:172–181. [PubMed: 16204703]
20. Sweet SMM, Bailey CM, Cunningham DL, Heath JK, Cooper HJ. Large scale localization of protein phosphorylation by use of electron capture dissociation mass spectrometry. Mol Cell Proteomics. 2009; 8:904–912. [PubMed: 19131326]
21. Boersema PJ, Mohammed S, Heck AJR. Phosphopeptide fragmentation and analysis by mass spectrometry. J Mass Spectrom. 2009; 44:861–878. [PubMed: 19504542]
22. Ge Y, Rybakova IN, Xu QG, Moss RL. Top-down high-resolution mass spectrometry of cardiac myosin binding protein C revealed that truncation alters protein phosphorylation state. Proc Natl Acad Sci U S A. 2009; 106:12658–12663. [PubMed: 19541641]
23. Zhang J, Guy MJ, Norman HS, Chen YC, Xu QG, Dong XT, Guner H, Wang SJ, Kohmoto T, Young KH, Moss RL, Ge Y. Top-down quantitative proteomics identified phosphorylation of cardiac troponin I as a candidate biomarker for chronic heart failure. J Proteome Res. 2011; 10:4054–4065. [PubMed: 21751783]
24. Dong XT, Sumandea CA, Chen YC, Garcia-Cazarin ML, Zhang J, Balke CW, Sumandea MP, Ge Y. Augmented phosphorylation of cardiac troponin I in hypertensive heart failure. J Biol Chem. 2012; 287:848–857. [PubMed: 22052912]
25. Ayaz-Guner S, Zhang J, Li L, Walker JW, Ge Y. In vivo phosphorylation site mapping in mouse cardiac troponin I by high resolution top-down electron capture dissociation mass spectrometry: Ser22/23 are the only sites basally phosphorylated. Biochemistry. 2009; 48:8161–8170. [PubMed: 19637843]
26. Peng Y, Chen X, Zhang H, Xu QG, Hacker TA, Ge Y. Top-down targeted proteomics for deep sequencing of tropomyosin isoforms. J Proteome Res. 2013; 12:187–198. [PubMed: 23256820]
27. Jin YT, Peng Y, Lin ZQ, Chen YC, Wei LM, Hacker TA, Larsson L, Ge Y. Comprehensive analysis of tropomyosin isoforms in skeletal muscles by top-down proteomics. J Muscle Res Cell Motil. 2016; 37:41–52. [PubMed: 27090236]
28. Yu DY, Peng Y, Ayaz-Guner S, Gregorich ZR, Ge Y. Comprehensive characterization of AMP-activated protein kinase catalytic domain by top-down mass spectrometry. J Am Soc Mass Spectrom. 2016; 27:220–232. [PubMed: 26489410]
29. Peng Y, Gregorich ZR, Valeja SG, Zhang H, Cai WX, Chen YC, Guner H, Chen AJ, Schwahn DJ, Hacker TA, Liu XW, Ge Y. Top-down proteomics reveals concerted reductions in myofilament and z-disc protein phosphorylation after acute myocardial infarction. Mol Cell Proteomics. 2014; 13:2752–2764. [PubMed: 24969035]
30. Pesavento JJ, Mizzen CA, Kelleher NL. Quantitative analysis of modified proteins and their positional isomers by tandem mass spectrometry: Human histone H4. Anal Chem. 2006; 78:4271–4280. [PubMed: 16808433]
31. Zabrouskov V, Ge Y, Schwartz J, Walker JW. Unraveling molecular complexity of phosphorylated human cardiac troponin I by top down electron capture dissociation/electron transfer dissociation mass spectrometry. Mol Cell Proteomics. 2008; 7:1838–1849. [PubMed: 18445579]
32. Creese AJ, Cooper HJ. The effect of phosphorylation on the electron capture dissociation of peptide ions. J Am Soc Mass Spectrom. 2008; 19:1263–1274. [PubMed: 18585055]
33. Lopez-Clavijo AF, Duque-Daza CA, Creese AJ, Cooper HJ. Electron capture dissociation mass spectrometry of phosphopeptides: Arginine and phosphoserine. Int J Mass Spectrom. 2015; 390:63–70.

34. Zhang J, Dong X, Hacker TA, Ge Y. Deciphering modifications in swine cardiac troponin I by top-down high-resolution tandem mass spectrometry. J Am Soc Mass Spectrom. 2010; 21:940–948. [PubMed: 20223681]
35. Xu FM, Xu QG, Dong XT, Guy M, Guner H, Hacker TA, Ge Y. Top-down high-resolution electron capture dissociation mass spectrometry for comprehensive characterization of post-translational modifications in rhesus monkey cardiac troponin I. Int J Mass Spectrom. 2011; 305:95–102.
36. Guner H, Close PL, Cai WX, Zhang H, Peng Y, Gregorich ZR, Ge Y. MASH Suite: a user-friendly and versatile software interface for high-resolution mass spectrometry data interpretation and visualization. J Am Soc Mass Spectrom. 2014; 25:464–470. [PubMed: 24385400]
37. Cai WX, Guner H, Gregorich ZR, Chen AJ, Ayaz-Guner S, Peng Y, Valeja SG, Liu XW, Ge Y. MASH Suite Pro: a comprehensive software tool for top-down proteomics. Mol Cell Proteomics. 2016; 15:703–714. [PubMed: 26598644]
38. Iavarone AT, Paech K, Williams ER. Effects of charge state and cationizing agent on the electron capture dissociation of a peptide. Anal Chem. 2004; 76:2231–2238. [PubMed: 15080732]
39. Krusemark CJ, Frey BL, Belshaw PJ, Smith LM. Modifying the charge state distribution of proteins in electrospray ionization mass spectrometry by chemical derivatization. J Am Soc Mass Spectrom. 2009; 20:1617–1625. [PubMed: 19481956]
40. Liu J, Konermann L. Irreversible thermal denaturation of cytochrome c studied by electrospray mass spectrometry. J Am Soc Mass Spectrom. 2009; 20:819–828. [PubMed: 19200750]

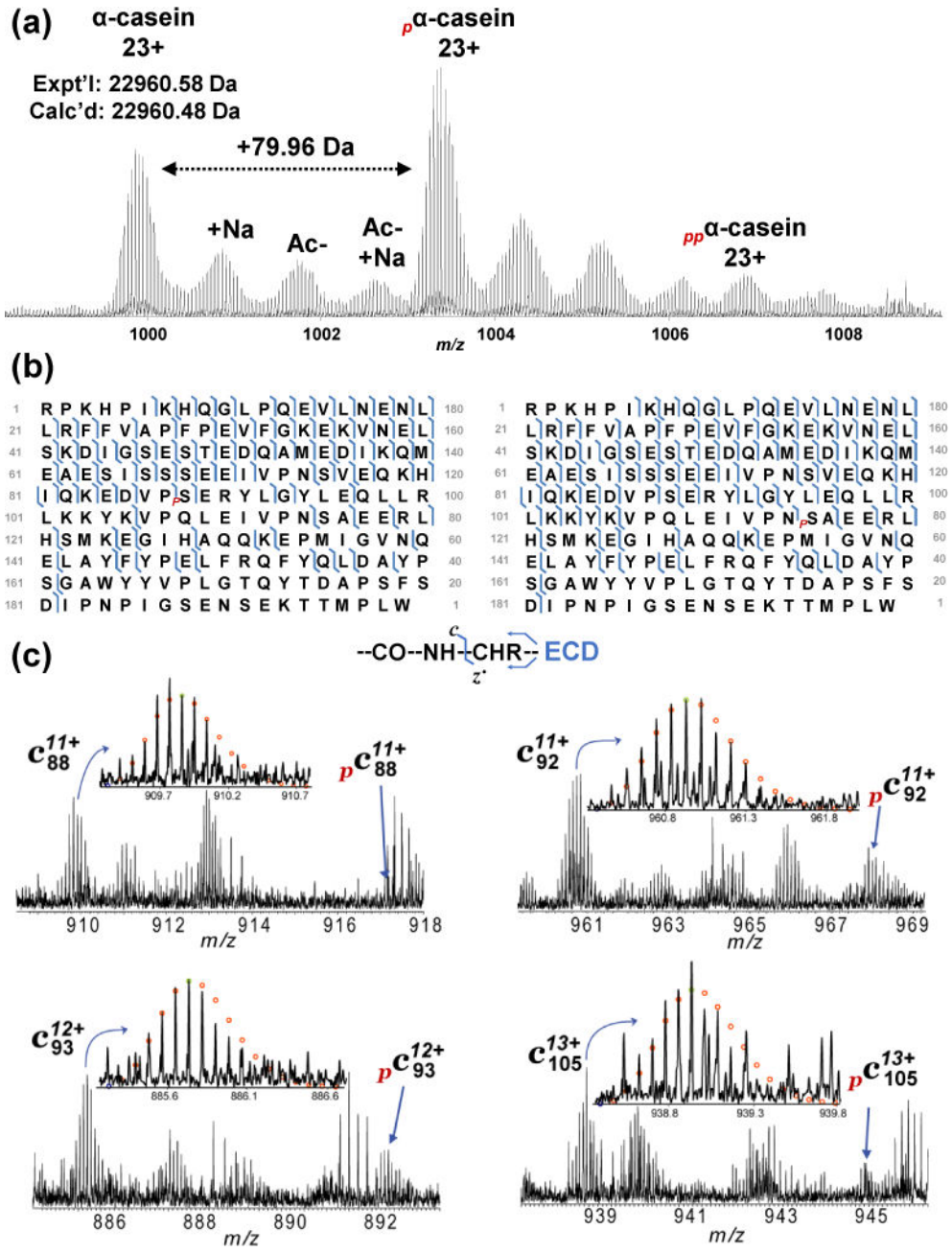

Figure 1.

(a) FTMS spectrum of α-casein. +22 Da, +42 Da, and +64 Da, represent possible sodium adduct, acetylation, acetylation with sodium adduct, respectively; $_p$, and $_{pp}$, mono- and bis-phosphorylation, respectively. (b) Fragmentation maps of the monophosphorylated α-casein by electron capture dissociation (ECD), which match the sequence from UniProt (UniProtKB-P02662), with phosphorylation on Ser88 (left) or Ser115 (right), respectively. (c) Representative ECD fragment ions demonstrating the coexistence of mono-phosphorylated isomers

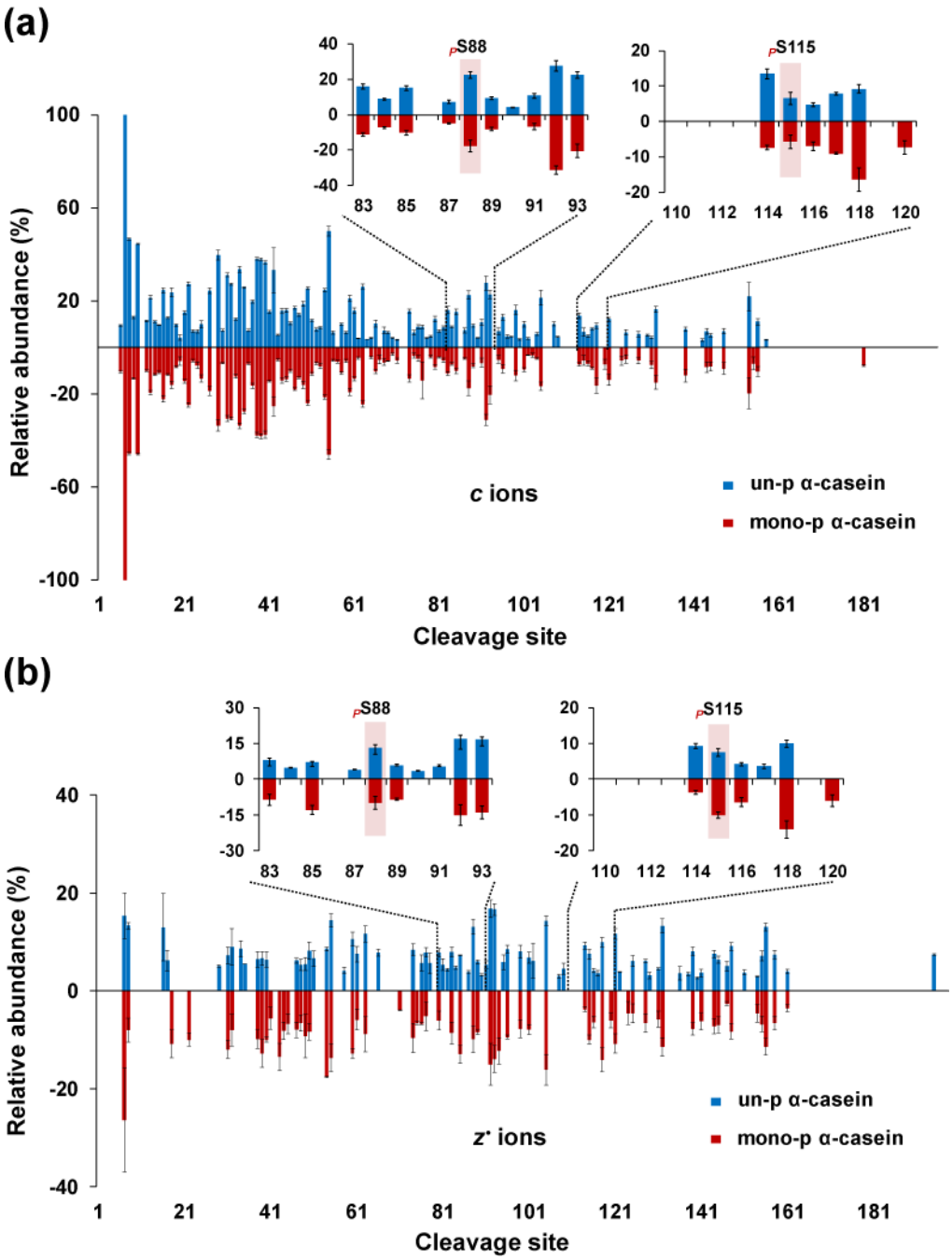

Figure 2.

Statistical comparison of ECD fragments of un- and mono-phosphorylated α-casein (23^+) at Ser115. The relative intensity of ***c*** ions (a), and $\boldsymbol{z}^{\bullet}$ ions (b) are plotted versus the cleavage site in the amino acid sequence. The blue bars (upper) represent unphosphorylated α-casein fragments from ECD, and the red bars (lower) represent mono-phosphorylated α-casein fragments from ECD. The standard error was calculated for each fragment based on nine spectra

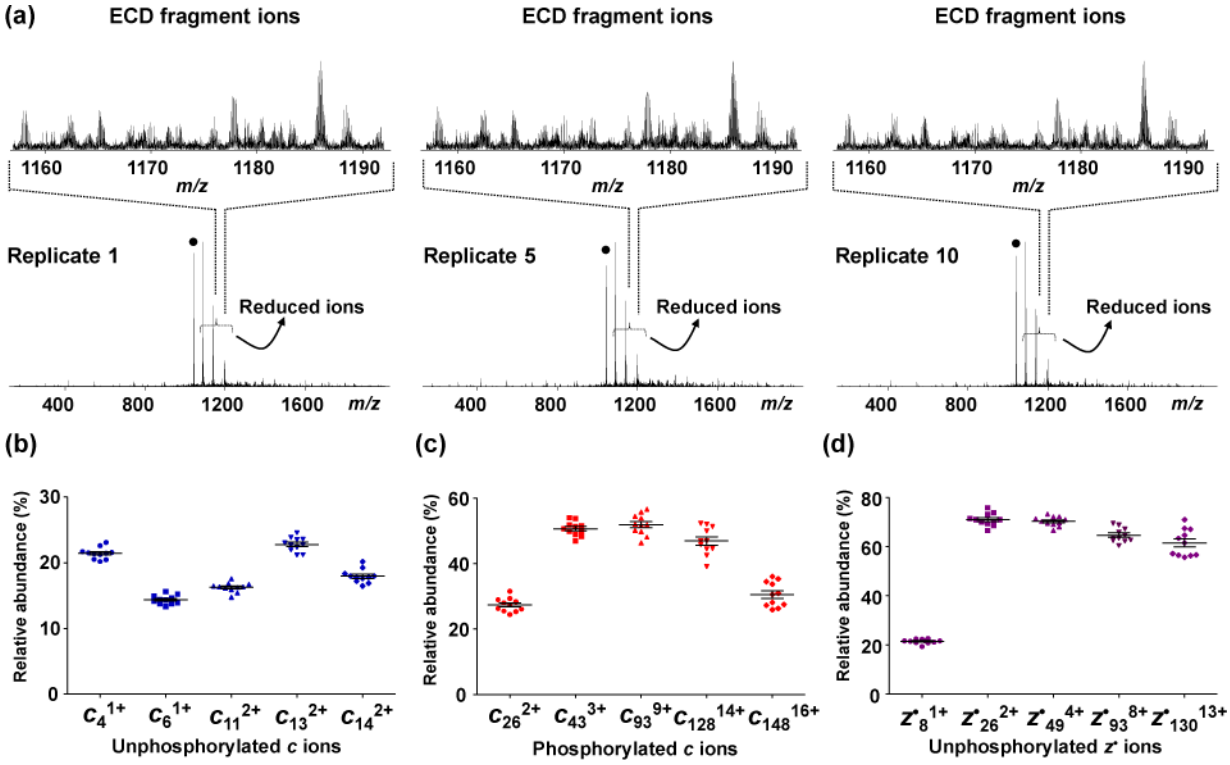

Figure 3.

Evaluation of the reproducibility of ECD fragmentation. (a) Three representative ECD spectra from fully phosphorylated β- casein (23^{+}, indicated by ●) with 0.8 eV electron energy and 50 ms electron irradiation time from 10 replicates; insert, zoom-in view of the ECD fragments. (b)–(d) The normalized abundance of representative ions were plotted across all 10 replicates for unphosphorylated ***c*** ions, phosphorylated ***c*** ions, unphosphorylated $\boldsymbol{z}^{\bullet}$ ions, respectively. The black bars indicate the standard error of the mean

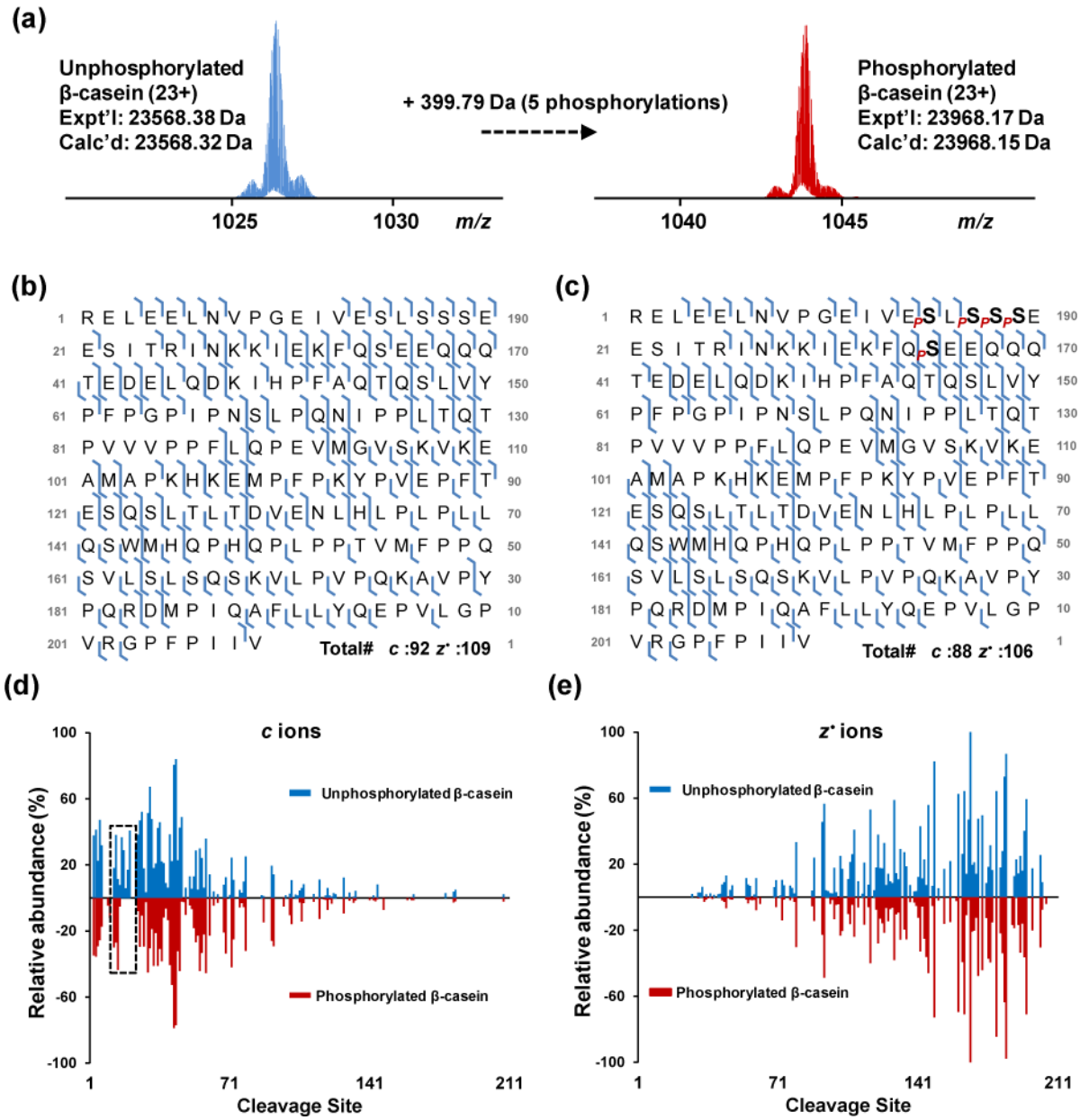

Figure 4.

Fragmentation maps and comparison of relative abundance of the product ions from unphosphorylated and phosphorylated β-casein. (a) MS isolation of charge state 23^+ of the unphosphorylated (left) and the multi-phosphorylated β-casein (right) before ECD experiments. ECD fragmentation maps of the charge states 23^+ of the unphosphorylated (b) and the phosphorylated β- casein (c) using the "standard" ECD conditions, which match the sequence from UniProt (UniProtKB-P02666). *p* indicates the phosphorylation sites (Ser15, Ser17, Ser18, Ser19, and Ser35). The relative intensity of ***c*** ions (d), and $\boldsymbol{z}^{\bullet}$ ions (e) are plotted against the cleavage sites in the amino acid sequence. The blue bars (upper) represent the unphosphorylated β-casein fragments, and the red bars (lower) represent the phosphorylated β-casein fragments

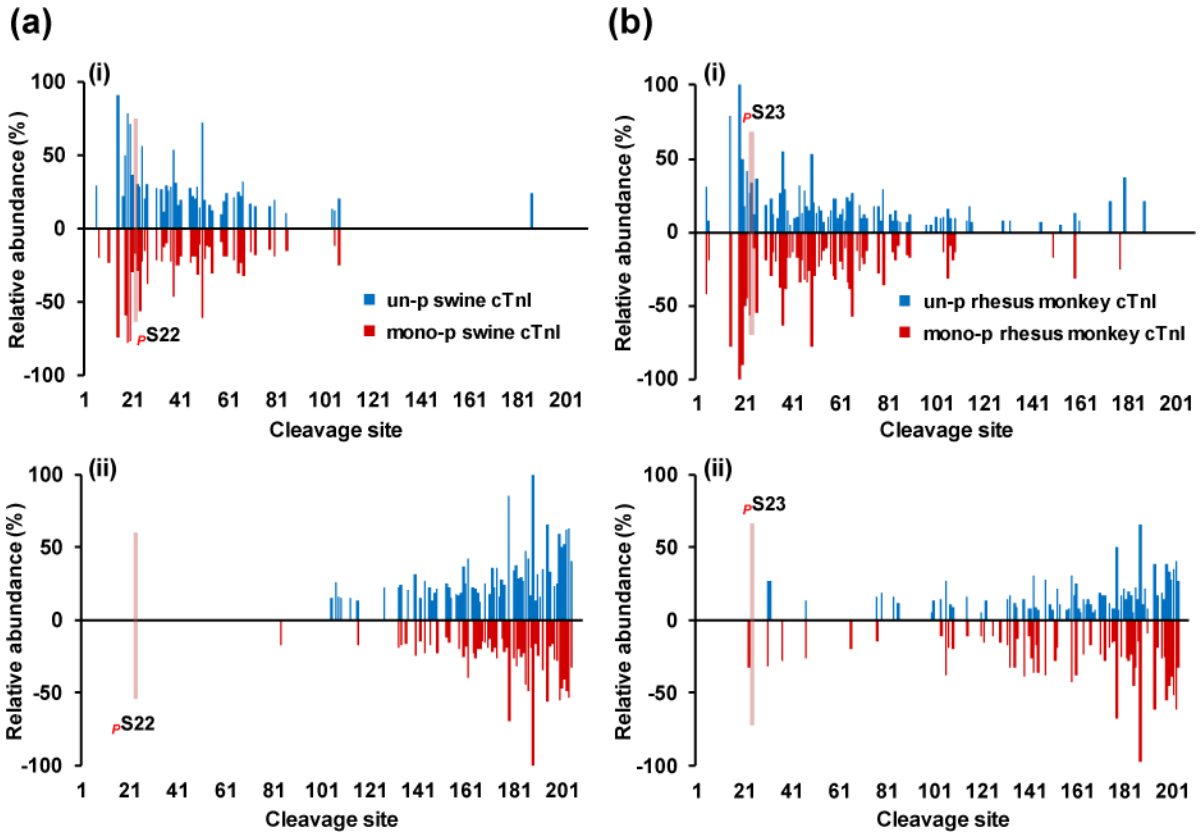

Figure 5.

Comparison of the ECD fragments of un- and mono-phosphorylated (a) swine cardiac troponin I (cTnI) and (b) rhesus monkey cTnI. The normalized intensity of the ***c*** fragment ions (i) and the $z^{\bullet}$ fragment ions (ii) are plotted versus the cleavage site in the amino acid sequence. The matched sequences were from UniProt (UniProtKB-A5X5T5 with N-terminal acetylation and V116A variance) for swine cTnI, and (UniProtKB-A0A1D5RFH2 with N-terminal acetylation) for rhesus monkey cTnI. The upper part (blue bars) represents fragments from the unphosphorylated form; the lower part (red bars) represents fragments from the monophosphorylated form. The phosphorylation sites of the swine cTnI and the rhesus monkey cTnI are Ser22 and Ser23, respectively